Photoionization of As_2 and As_4: Implications for group V clusters

R. K. Yoo, B. Ruscic, and J. Berkowitz
Chemistry Division, Argonne National Laboratory, Argonne, Illinois 60439

(Received 27 November 1991; accepted 27 January 1992)

The vacuum ultraviolet photoionization mass spectrum of As_4 is presented, from the ionization threshold to 600 Å. The apparent adiabatic ionization potential is $\leqslant 8.49$ eV, but the true value may be significantly lower. Three broad autoionization features are observed, probably comprising members of a Rydberg series converging to the $\tilde{B}\,^2A_1$ state of As_4^+. The first fragment, As_3^+, has an appearance potential (0 K) of 11.23 ± 0.05 eV, from which we extract $\Delta H^0_{f_0}(As_3^+) \leqslant 228.7 \pm 1.3$ kcal/mol. The photoion yield curve of As_2^+ (As_2) is obtained under conditions where As_2 is dominant in the vapor. The adiabatic ionization potential is 9.69 ± 0.02 eV. Two prominent autoionizing Rydberg series are observed, converging to the $A\,^2\Sigma_g^+$ state of As_2^+, with an ionization potential of 10.238 ± 0.002 eV. At higher energy, three members of a window resonance series can be seen, converging to the $B\,^2\Sigma_u^+$ state of As_2^+, with an ionization potential of 15.37 eV. From an upper limit to the partial pressure of As_3, equilibrium conditions, and assuming a triangular As_3, we deduce $\Delta H^0_{f_0}(As_3) \geqslant 60.0$ kcal/mol; other criteria suggest $\Delta H^0_{f_0}(As_3) \cong 63$ kcal/mol. Consequently, the adiabatic ionization potential of As_3 is < 7.32 eV, and probably $\leqslant 7.19$ eV. Several implications are drawn, relevant to recent studies of antimony and bismuth clusters.

I. INTRODUCTION

The development of supersonic expansion techniques in recent years has provided a major impetus to the study of elemental clusters. The types of clusters which have been generated can be categorized according to the strength (D) of the chemical bonds that are formed. Thus the van der Waals bonding in clusters of the noble gases can be characterized with $D < 0.1$ eV; hydrogen bonded clusters, and/or ionic clusters bound by a charge-induced dipole interaction may have $D \approx 0.1$–0.3 eV; and clusters involving chemical bonding may have $D > 1$ eV. This is admittedly a crude categorization, since, e.g., clusters of the IIa or IIb metals, such as Be and Hg, have very weak bonds as dimers, but may develop much stronger bonds in larger clusters. Nevertheless, it is useful to keep these distinctions in mind.

A major problem in cluster studies of neutral species is the preparation of a specific cluster, in the absence of other clusters. The identification of a given cluster is most often achieved by some form of mass analysis of the corresponding charged species. For example, a distribution of clusters may be ionized by a pulsed laser, and examined by time-of-flight (TOF) mass spectrometry. Due to possible fragmentation processes, there need not be a unique correlation between the properties (wavelength dependence, abundance) of a neutral species and the cation of the same nominal mass. If specific clusters can be generated, the fragmentation problem can, in principle, be solved. The unique properties of each cluster can then be utilized in further studies, e.g., in analytical detection. Thus Bock and Müller[1] have examined the $P_4 \rightleftarrows 2P_2$ equilibrium using the characteristic photoelectron spectrum of each species as a measure of its abundance. Several examples of such elemental clusters, formed without the benefit of supersonic expansion, exist in nature. They tend to be members of Group IV (C_n, Si_n, Ge_n), Group V (P_n, As_n, Sb_n), and Group VI (S_n, Se_n, Te_n), and clearly belong to the strong bonding category. By appropriate control of pressure, temperature, and chemical activity, it is possible to adjust the vapor composition to emphasize different sizes of clusters in these systems. This may sometimes result in practical benefits. For example, it has been found that higher quality crystals of GaAs are formed when the arsenic vapor contains As_2, rather than As_4.[2] Our present purpose is to investigate the photoionization behavior of the individual arsenic species.

When solid arsenic is sublimed, the dominant vapor species is As_4. Upon superheating, or providing for diminished partial pressure by using some arsenic compound, it is possible to have As_2 as the major vapor species, and ultimately atomic As. However, the thermal stability of As_3 is such that it never attains a significant relative abundance under equilibrium conditions. Nevertheless, we shall demonstrate that it is possible to establish some plausible range for its heat of formation and its adiabatic ionization potential.

The He I photoelectron spectrum of As_4 has been reported by several groups[3–6] in the past two decades, each time with improved resolution. Three of these groups[4,5,7] have also reported the photoelectron spectrum of As_2, and one[5] has obtained the photoelectron spectrum of atomic As. The Berkeley group,[6,7] using supersonic expansion cooling of the vapor, was the only one able to observe vibrational structure in As_4 and As_2. Some photoionization mass spectrometric studies have been performed on P_4 (Ref. 8) and P_2 (Ref. 9), but none on As_4 and As_2. Earlier, a photoionization mass spectrometric study of atomic As was conducted in our laboratory.[10] The spectrum displayed sharp autoionization structure in the near threshold region, and a prominent window resonance series in a higher energy region corresponding to photoexcitation of an electron from the 4s orbital.

 0021-9606/92/096696-14$06.00

II. EXPERIMENTAL ARRANGEMENT

The photoionization apparatus utilized in these experiments was a reincarnation of an older apparatus. The essential components are a 1 m, normal incidence vacuum ultraviolet monochromator (McPherson), and a magnetic mass spectrometer. The sample is loaded into a Mo oven, and radiatively heated by a tungsten filament. The temperature of the oven is monitored by a Pt–Pt, 10% Rh thermocouple. A crude molecular beam of the vapor is formed when the effusive flow from the oven is intercepted by radiation and cooling shields containing slits. The molecular beam is crossed by a selected bandwidth of the photon beam within an "open" ionization chamber, and the resulting photoions are forced out by a repeller field. The molecular, photon, and ion beams are mutually orthogonal in space. The photoion beam is accelerated, focused by an electrostatic quadrupole lens, and mass analyzed. A particle multiplier pulse counts the ion signal, while a Ni photocathode monitors the light intensity. The analog photoelectric current is converted to a voltage, and then to pulses by a voltage to frequency converter, and digitally counted. The wavelength response of the Ni photocathode had previously been calibrated. The wavelength resolution was adjusted for specific experiments between 0.83 and 2.5 Å FWHM.

A molecular beam of essentially pure As_4 was generated upon heating a sample of crystalline arsenic to ~300 °C. A beam containing mostly As_2 (As_2:As_4 ≈3:1) was formed in the vapor above a sample of InAs, at a temperature of ~600 °C. The contribution of As^+ and As_2^+ from As_4 to the As^+ and As_2^+ signals from As_2, which could be evaluated, was negligible. The As and InAs samples were of commercial origin and were used without further purification.

III. EXPERIMENTAL RESULTS

A. Photoionization of As_4

An overview of the photoionization mass spectrum of As_4 appears in Fig. 1. It is very similar in gross features to the photoionization mass spectrum of P_4.[8] The parent ion is dominant throughout the spectrum. The first fragment, As_3^+, initially appears at $\lambda \approx 1100$ Å, followed by As_2^+ ($\lambda > 1000$ Å) and finally As^+, at $\lambda \approx 850$ Å.

1. As_4^+ from As_4

In Fig. 1, three resonancelike features are evident in the As_4^+ curve, centered at ~1338, ~1240, and ~1197 Å. They become progressively narrower with decreasing wavelength. This is partly due to the distortion that occurs with a λ display, i.e., $\Delta\lambda \propto \lambda^2 \Delta E$, but representative energy widths for these resonances still decline, with $\Delta E \sim 0.48$ eV (1338 Å), ~0.33 eV (1240 Å), and ~0.21 eV (1197 Å). Similar features appear in the spectrum of P_4^+ (P_4).[8] In this latter work, Smets *et al.*[8] claim to observe several more, sharper peaks at successively shorter wavelengths, but we shall try to show below that we think this is unlikely, and that these

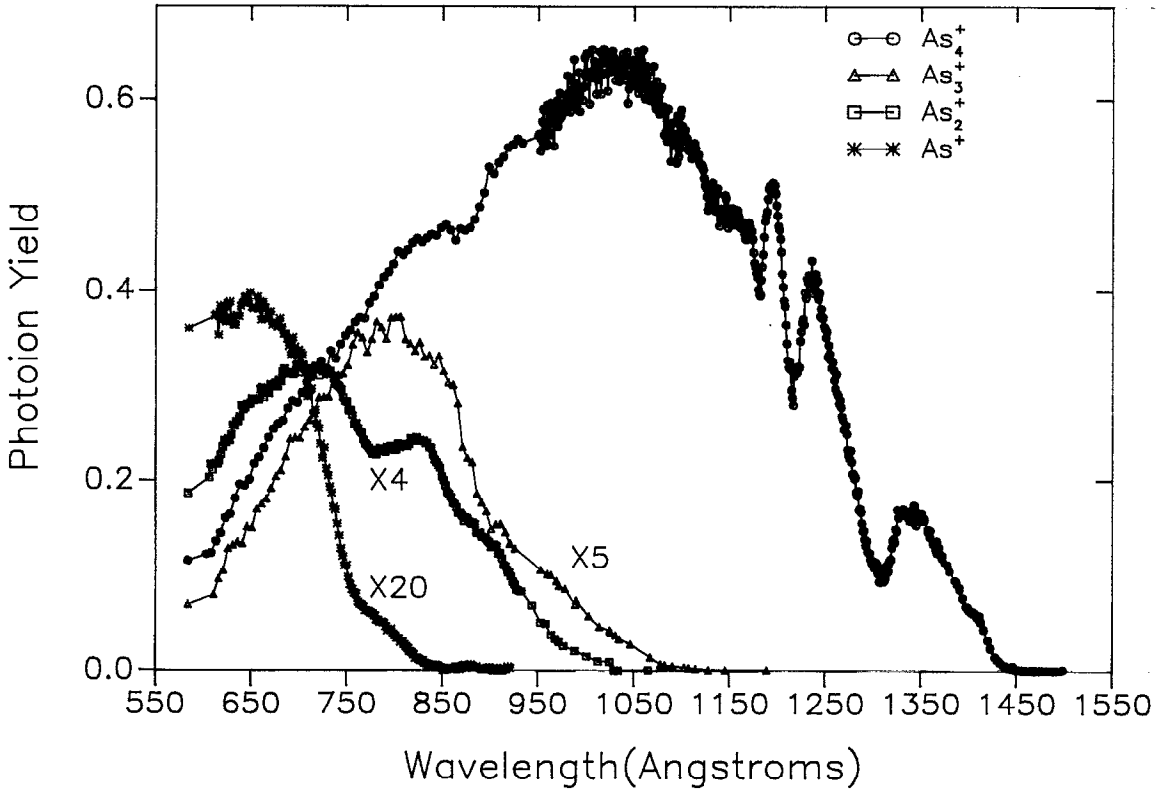

FIG. 1. An overview of the photoion yield curves of As_4^+, As_3^+, As_2^+, and As^+ from As_4. The ordinate is in arbitrary units, but the relative intensities are significant.

peaks may be artifacts due to a noisy signal in a region of weak light intensity.

In P_4 and As_4, both tetrahedral,[11] the uppermost occupied orbitals may be written[6] $(a_1)^2(t_2)^6(e)^4$. These 12 electrons represent the molecular interaction of 3 p-type electrons per atom. Smets *et al.*[8] assign the autoionization structure in P_4 to Rydberg members converging on a $^2A_1$ state, i.e., $(a_1)^2(t_2)^6(e)^4 + h\nu \rightarrow \cdots a_1(t_2)^6(e)^4 nl \rightarrow \cdots a_1(t_2)^6(e)^4, {}^2A_1 + e$. They elaborate this picture by claiming to see three series, converging to the three most intense vibrational levels in the $\tilde{B}\,^2A_1$ state observed in the photoelectron spectrum of P_4.[12,13] If this were indeed the case, one would expect to see vibrationally resolved bands within each of the first three broad bands, rather than their sudden appearance in the higher Rydberg members. Such vibrational fine structure is not apparent in the first three bands of P_4, nor is it in As_4.

The best resolved photoelectron spectra of both P_4 and As_4 are contained in the recent papers of Wang *et al.*[6] For P_4, they report a vertical and an adiabatic IP (ionization potential) for the $\tilde{B}\,^2A_1$ state, which differ by only one vibrational quantum. If each of the first three broad bands in the photoionization spectrum of P_4 corresponds to a Rydberg band, encompassing several unresolved vibrations, then the peaks of these bands should converge to the peak in the photoelectron spectrum, i.e., the vertical IP. In Table I, we have tested this hypothesis by calculating the effective quantum numbers corresponding to the peaks of these three bands. The quantum defect is not very constant in this limited series. Surprisingly, it becomes much more constant if we choose the limit to be the adiabatic IP for the $\tilde{B}\,^2A_1$ state of P_4^+.

Applying the same approach to the three broadbands in As_4, we note that neither the vertical nor the adiabatic IP given by Wang *et al.*[6] for $\tilde{B}\,^2A_1$ of As_4^+ yields constant quantum defects, but the situation improves if we choose as a limit one or both of the bands labeled in their figure as hot bands. This is circumstantial, and not very conclusive evidence that the adiabatic threshold for formation of the $\tilde{B}\,^2A_1$ state of As_4^+ may be lower than the value selected by Wang *et al.*[6] However, this inference is not very pleasing, for it implies that the peak in each band is correlated by the Rydberg formula to the first vibrational member in the photoelectron spectrum. If this were true, the higher vibrational bands in each Rydberg electronic state would not autoionize as effectively as $v' = 0$. There is no obvious reason why this should be so.

Figure 1 shows that the photoion yield curve of As_4^+ (As_4) approaches the background level gradually, at $\sim$1450 Å. A magnified view of the threshold region appears in Fig. 2. Here we see that the last significant signal above background occurs between $\sim$1440–1460 Å. At the extreme, this implies an *apparent* adiabatic threshold of $\sim$8.49 eV. In the photoelectron spectrum of As_4, Wang *et al.*[6] observe a doublet consequent upon electron emission from the uppermost occupied orbital, which is doubly degenerate (e). The resulting cation is subject to Jahn–Teller distortion, giving rise to the doublet. Their photoelectron spectrum appears to reach the background level at $\sim$8.3 eV. However, their Jahn–Teller analysis leads to the prediction that the true adiabatic threshold is much lower still, 7.83 eV.

It seems quite certain that the ground state of As_4^+ is substantially distorted from a tetrahedral structure, and hence the Franck–Condon region will be broad, and gradually diminish toward threshold. On the other hand, the temperature of the vapor allows for the possibility of hot bands (viz. their attribution of two vibrational components in the $^2A_1$ region to hot bands), and this possibility can extend the observed onset to lower energies. Neither the PIMS nor the PES experiments alone can be used to infer the true adiabatic IP of As_4. Either one must invoke some model (such as the Jahn–Teller analysis of Wang *et al.*[6]) or a completely different experiment, such as charge exchange bracketing in an ICR cell or a flow tube must be utilized to arrive at the true, adiabatic IP.

2. As_3^+ from As_4

The photoion yield curve of As_3^+ (As_4) exhibits a kink, or change of slope, at about 900 Å (see Fig. 1), but in other ways is not remarkable. The threshold region for the formation of As_3^+ from As_4 is amplified in Fig. 3. The tail of the photoion yield curve intersects the base line at 1128 ± 5 Å $\equiv 10.99 \pm 0.05$ eV. The internal (vibrational plus rotational) energy of As_4 at 500 K is 0.242 eV.[14] The inferred 0 K threshold is calculated[15] to be 11.23 eV. Taking $\Delta H^0_{f_0}(As_4) = 38.5 \pm 0.6$ kcal/mol (Ref. 16) and

TABLE I. Rydberg series members observed in P_4 and As_4.

P_4			VIP = 11.847(3)[a]		AIP = 11.776(3)[a]	
λ_n (Å)		E_n (eV)	n^*		n^*	
1244		9.967	2.690		2.742	
1148		10.800	3.605		3.734	
1110		11.170	4.482		4.738	
As_4						
λ_n (Å)	E_n (eV)	VIP = 11.058(3)[a]	AIP = 11.017(3)[a]	HB1 = 10.973_6[a]		HB2 = 10.930_3[a]
		n^*	n^*	n^*		n^*
1338	9.266	2.756	2.788	2.823		2.860
1240	10.00	3.586	3.658	3.738		3.824
1197	10.358	4.409	4.544	4.701		4.876

[a] Assumed limits: VIP = vertical IP; AIP = adiabatic IP; HB = hot band from Ref. 6.

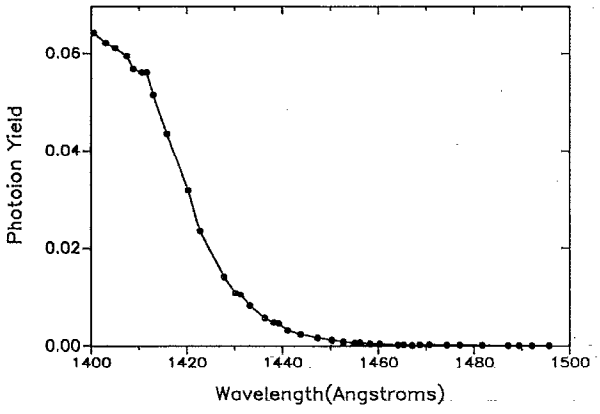

FIG. 2. A magnified version of the threshold region of the As_4^+ (As_4) photoion yield curve.

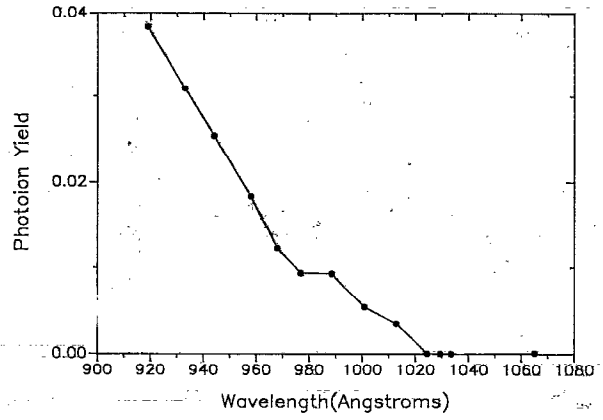

FIG. 4. The threshold region of the As_2^+ (As_4) photoion yield curve.

$\Delta H^0_{f_0}(As) = 68.8$ kcal/mol,[17] we deduce $\Delta H^0_{f_0}(As_3^+) \leqslant 228.7 \pm 1.3$ kcal/mol.

3. As_2^+ from As_4

The photoion yield curve of As_2^+ (As_4) shown in Fig. 1 has a kink at about 900 Å, and a distinct dip to a local minimum at ~780 Å. The threshold region for this process is displayed in Fig. 4. There appears to be a change of slope at about 975 Å. The curve intersects the base line at $\sim 1025 \pm 2$ Å $\equiv 12.096 \pm 0.024$ eV. The inferred 0 K appearance potential is 12.338 ± 0.024 eV, or 284.5 ± 0.6 kcal/mol. The adiabatic ionization potential of As_2 (see Sec. III B 1 below) is 9.69 ± 0.02 eV $\equiv 223.5 \pm 0.5$ kcal/mol. Therefore, for the dissociation of As_4 into two As_2 moieties, we deduce $\Delta H_0 \leqslant 61.0 \pm 0.8$ kcal/mol. Earlier thermochemical equilibrium studies[17] had arrived at 54 ± 1 kcal/mol for this quantity. Therefore, the photoionization threshold appears to be subject to a kinetic shift of 7 kcal/mol.

Smets *et al.*,[8] studying the photodissociative ionization of P_4 to P_2^+, had concluded that their appearance potential, together with the ionization potential of P_2, yielded a decomposition energy ($P_4 \rightarrow 2P_2$) of 54.77 kcal/mol at 0 K, virtually identical with the thermochemical value (54.3 ± 1.2 kcal/mol). However, they used an adiabatic ionization potential of P_2 from Carrol and Mitchell, since shown to be too high.[9] Our analysis of their data gives $\leqslant 56.9 \pm 0.7$ kcal/mol, equivalent to a kinetic shift of 2.6 ± 1.4 kcal/mol.

4. As^+ from As_4

Figure 5 is an expanded view of the ion yield curve of the threshold region for this process. A change of slope is evident at ~760 Å. Since this is the third fragment, it may be expected to exhibit a substantial kinetic shift. The observed intersection of the curve with the background level occurs at 835 ± 3 Å $\equiv 14.85 \pm 0.05$ eV, or at 0 K, 15.09 ± 0.05 eV. If we assume that this process corresponds to successive decomposition, i.e., $As_4^+ \rightarrow As_2^+ \rightarrow As^+$, we can compute the onset from the decomposition energy for $As_4 \rightarrow 2As_2$ ($\Delta H_0 = 54.3 \pm 1$ kcal/mol), $D_0(As_2) = 3.96$ eV (Ref. 19) and IP (As) $= 9.7886 \pm 0.0002$ eV (Ref. 20) to be 16.10 eV. Since our observed threshold is ~1 eV lower, we can conclude that the process near threshold must correspond to

$$As_4 + h\nu \rightarrow As^+ + As_3 + e.$$

Hence, we can deduce an upper limit for $H^0_{f_0}(As_3)$. From previously noted values for $\Delta H^0_{f_0}(As_4)$, $\Delta H^0_{f_0}(As)$, and IP (As), we obtain $\Delta H^0_{f_0}(As_3) \leqslant 92.0$ kcal/mol. The true value may be expected to be substantially lower.

B. Photoionization of As_2

The photoionization mass spectrum of the vapor from the InAs sample had a ratio of $As_2^+ : As_4^+ > 3:1$ at several

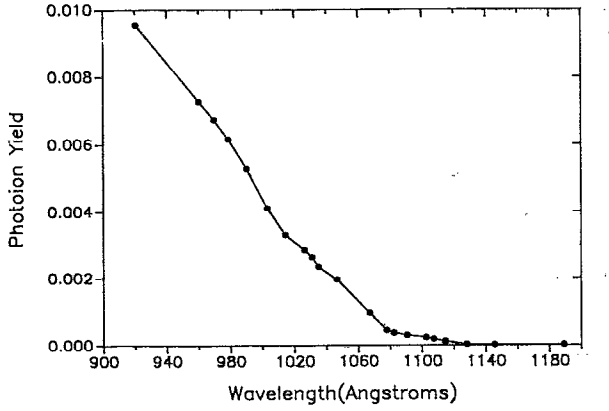

FIG. 3. The threshold region of the As_3^+ (As_4) photoion yield curve.

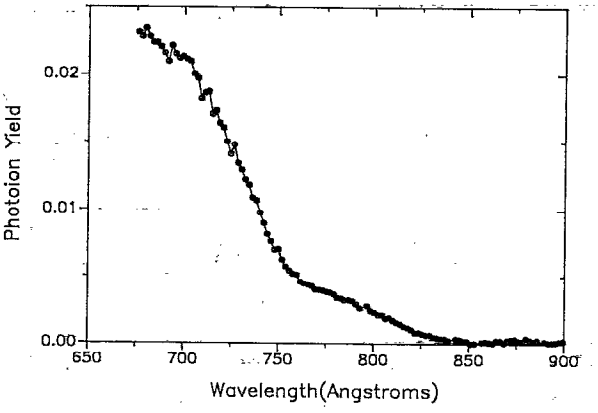

FIG. 5. The threshold region of the As^+ (As_4) photoion yield curve.

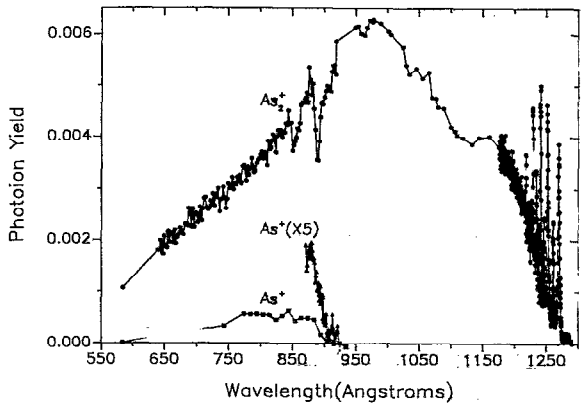

FIG. 6. An overview of the photoion yield curves of As_2^+ and As^+ from As_2. The relative intensities are significant.

wavelengths. Since the fragment As_2^+ from As_4 (see Fig. 1) is more than five times weaker than As_4^+ from As_4 at $\lambda > 750$ Å, the photoion yield curve of As_2^+ (As_2) from the InAs sample has a contribution from As_4, which was $< 6.7\%$ for $\lambda > 750$ Å, and vanishes for $\lambda > 1025$ Å. An overview of the photoionization mass spectrum of As_2 is shown in Fig. 6. The parent ion dominates; As^+ (As_2) appears weakly, with an onset at ~ 925 Å. The parent ion displays two regions of autoionization resonance structure—peaks in the threshold region, and a few members of a window resonance series below ~ 900 Å.

1. $As_2^+(As_2)$ in the threshold region

An expanded view of the threshold region is shown in Fig. 7. The intensities of the autoionization peaks alternate, implying the presence of two series. The wavelengths of the series members are given in Table II.

The valence electronic configuration of As_2 is

$$(\sigma_g 4s)^2(\sigma_u 4s)^2(\sigma_g 4p)^2(\pi_u 4p)^4.$$

This is borne out by the He I photoelectron spectrum,[7] which reveals long vibrational progressions near threshold, resulting from the removal of an electron from the strongly bonding π_u orbital, and forming As_2^+ in the $X\,^2\Pi_{u,3/2}$ and $^2\Pi_{u,1/2}$ states. Ejection of an electron from the nominally bonding $\sigma_g 4_p$ orbital gives rise predominantly to the (0,0) peak for the $A\,^2\Sigma_g^+$ state of As_2^+. This characteristic behavior (broad Franck–Condon region for formation of $^2\Pi_u$, narrow Franck–Condon region for formation of $^2\Sigma_g^+$) is also observed in N_2, but the energy ordering of these orbitals is reversed. Only N_2^+ has an $X\,^2\Sigma_g^+$ ground state; for P_2^+, As_2^+, Sb_2^+, and Bi_2^+ the ground state is $X\,^2\Pi_{u,3/2}$.

Both the energy ordering and the sharpness of the autoionization peaks indicate that the two Rydberg series converge to the $A\,^2\Sigma_g^+$ state of As_2^+. Wang *et al.*[7] give the ionization potential for the process

$$As_2(X\,^1\Sigma_g^+) \rightarrow As_2^+(^2\Sigma_g^+)$$

as 10.230(5) eV. Using this limit, the energies E_n corresponding to the autoionization peaks λ_n and the Rydberg formula

$$E_n = \mathrm{IP} - \frac{R}{(n^*)^2},$$

where R is the Rydberg constant and n^* is the effective quantum number, we have calculated the n^* values corresponding to the observed λ_n, which we list in Table II. For a well-behaved Rydberg series, one expects the quantum defect ($n-n^*$) to remain approximately constant. From the n^* values calculated for IP = 10.230 eV, one can make out two series, corresponding to the stronger and weaker peaks. In both series, the quantum defect is gradually changing. By altering the limit to 10.238 eV (also given in Table II) one obtains a more nearly constant value of the quantum defect. Hence, we conclude that the IP for formation of As_2^+ ($A\,^2\Sigma_g^+$) is 10.238 ± 0.002 eV.

By dipole selection rules, one requires that

$$As_2(X\,^1\Sigma_g^+) + h\nu \rightarrow As_2^*(\text{ungerade})$$
$$\rightarrow As_2^+(^2\Sigma_g^+) + e(\text{ungerade}).$$

Consequently, the outgoing electron wave must correspond to $l = 1, 3, 5, \cdots$ and is most likely a p. By continuity, and also single electron selection rules, the Rydberg electrons should have p character. Theodosiou *et al.*[21] have calculated the p quantum defect for As in the Hartree–Slater approxi-

TABLE II. Autoionizing series in As_2 converging to $A\,^2\Sigma_g^+$.

λ_n (Å)	E_n (eV)	n^* (assuming IP = 10.230 eV)		n^* (assuming IP = 10.238 eV)	
1269.1	9.7695	5.4354		5.3888	
1260.5	9.8362		5.8778		5.8189
1251.7	9.9053	6.4730		6.3947	
1246.3	9.9483		6.9495		6.8529
1241.1	9.9899	7.5275		7.4052	
1237.9	10.0158		7.9697		7.8249
1234.3	10.0450	8.5756		8.3960	
1232.1	10.0629		9.0232		8.8146
1229.1	10.0875	9.7711		9.5078	
1226.9	10.1056		10.4578		10.1369
1225.7	10.1155	10.9005		10.5386	
1223.1	10.1370	12.0951		11.6062	
1217.9	10.1802	(16.5285)		(15.3421)	

mation, and obtained 2.4078. The quantum defect for our strong series is ~2.58, that for the weak series, ~2.15. A tentative interpretation for the two series, suggested by their relative intensities, is that the strong series corresponds to $np\pi$, the weaker one to $np\sigma$. The weighted mean of the respective quantum defects then comes close to the calculated p quantum defect. However, the reverse ordering of $np\sigma$ and $np\pi$ series has been inferred for P_2, and may apply here as well (see Sec. IV C).

The adiabatic ionization potential (i.e., that for formation of As_2^+, $X\,^2\Pi_{u,3/2}$) can be bracketed between the first observed autoionization peak at 1269.1 Å≡9.7695 eV, and the last predicted peak before the onset of autoionization. Taking $n^* = 5.8335$ for the first observed member of the weak series, the next prior member should occur at $n^* = 4.8335$, corresponding to $E_n = 9.6537$ eV≡1284.3 Å. Thus 9.65 eV < IP < 9.77 eV. Wang *et al.*[7] obtained 9.636(6) eV for this quantity from their high resolution photoelectron spectrum. This value is at least one vibrational quantum of As_2^+ (385 cm^{-1}≡0.0477 eV) too low. Wang *et al.* were faced with the deconvolution of two vibrational progressions ($^2\Pi_{u,3/2}$ and $^2\Pi_{u,1/2}$) together with hot bands appropriate to a temperature of 600 K. Their spectrum reveals relatively intense peaks below 9.65 eV, attesting to the influence of hot bands.

There is an underlying continuum below the autoionization peaks shown in Fig. 7, which is attributed to the formation of As_2^+, $X\,^2\Pi_{u,3/2}$ and $^2\Pi_{u,1/2}$. This underlying continuum diminishes toward threshold. It appears to have an onset at 1277–1280 Å≡9.686–9.709 eV. From this analysis, the adiabatic IP obtained by Wang *et al.* is one, or perhaps two vibrational quanta too low. We favor a value of 9.69 ± 0.02 eV.

2. $As_2^+(As_2)$ in the window resonance region (<900 Å)

Figure 8 is an expanded view of the photoion yield curve of As_2^+ (As_2). At least three members of a window resonance series are visible, with minima at 889.5, 850, and (834–834.5) Å. Our trial interpretation is that this series converges to a limit corresponding to the ejection of an electron from the next deeper orbital, $\sigma_u 4s$, and thus forming the

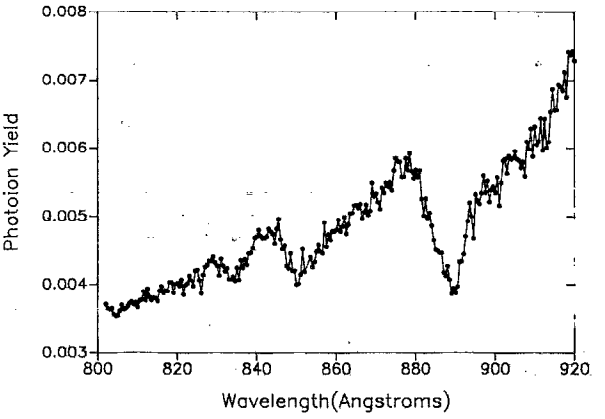

FIG. 8. An expanded view of the window resonance region in the photoion yield of As_2^+ (As_2).

$B\,^2\Sigma_u^+$ state of As_2^+. Of the three photoelectron spectra of As_2 that have been published only Elbel *et al.*[4] display the spectrum above ~12 eV. Elbel *et al.*[4] observe a very small peak at 15.32 eV, which they attribute to formation of a Σ_u state of As_2^+. With this limit and our observed minima, the Rydberg formula leads to $n^* = 3.138$, 4.306, and (5.475–5.422), i.e., the quantum defects are far from constant. With a revised limit of 15.37 eV, the values of n^* become 3.083, 4.167, and (5.152–5.197), which is more satisfactory.

In the photoionization process

$$As_2(X\,^1\Sigma_g^+) + h\nu \rightarrow As_2^+(B\,^2\Sigma_u^+) + e,$$

the outgoing electron must be gerade (i.e., $l = 0,2,\cdots$) according to electric dipole selection rules. By continuity and single electron selection rules, this must also be the case for the Rydberg electron. The probable Rydberg orbital is s-type. According to Theodosiou *et al.*,[21] the s quantum defect for As is 2.8665. If we assign $n = 6,7,8$ to the three series members observed, then $\delta_1 = 2.862$, 2.833, and (2.848–2.803), which is satisfactorily close to the calculated *atomic* As quantum defect. Hence, this analysis appears to be internally self-consistent. The relationship of this window resonance series to other atomic and homonuclear diatomic window resonance series is discussed in Sec. IV C and in another paper.[57]

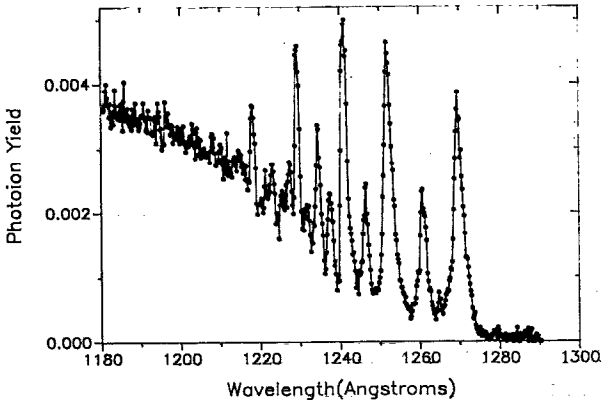

FIG. 7. An expanded view of the autoionization region near threshold in the photoion yield curve of As_2^+ (As_2).

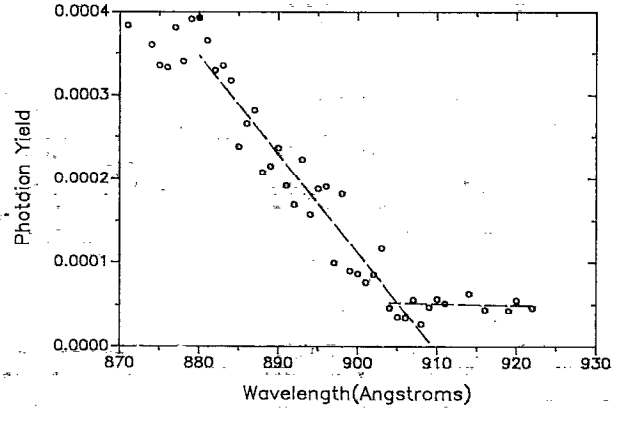

FIG. 9. The threshold region of the As^+ (As_2).

3. $As^+(As_2)$

The threshold region for formation of the fragment As^+ from As_2 is shown in an expanded form in Fig. 9. Within the statistical uncertainty, there is a quasilinear region from threshold to ~880 Å, below which the photoion yield curve reaches a plateau (and then declines below ~770 Å). The quasilinear portion intersects the background level at about 905.5 ± 5.0 Å $\equiv 13.69 \pm 0.08$ eV. The vibrational and rotational energy of As_2 at 900 K, which is available for dissociation, is 0.13 eV. Therefore, the 0 K threshold would be[15] 13.82 ± 0.08 eV. Since the ionization potential of As is 9.7886 ± 0.0002 eV,[20] an upper limit to $D_0(As_2)$ is 4.03 ± 0.08 eV. Huber and Herzberg[19] list $D_0(As_2) = 3.96$ eV, based upon a predissociation observed by Kinzer and Almy.[22] Thus the threshold observed here is not just an upper limit, but (within the statistical uncertainty) the true value.

C. Photoionization of As_3

An attempt was made to observe As_3^+ (As_3) during the experiments with the InAs sample which, though unsuccessful, provided a means of estimating a lower limit for $\Delta H^0_{f_0}(As_3)$.

We had noted earlier (Sec. III B) that the ratio of As_2 to As_4 above the InAs sample, measured at several wavelengths, was $\gtrsim 3{:}1$. An attempt was made to observe As_3^+ at a strong line, Lyman $\alpha = 1215.7$ Å $\equiv 10.2$ eV, during these experiments. At this wavelength, As_2^+ (As_2) has attained about half of its maximum cross section. We shall show that the ionization potential of As_3 is significantly lower than that of As_2 (and also As_4). Hence, if we assume a normally behaving photoionization cross section curve of As_3^+ (As_3), i.e., low near threshold, rising to a maximum a few eV above threshold, then declining, as is the case for As_2^+ (As_2) and As_4^+ (As_4), then the photoionization cross section for As_3^+ (As_3) should be substantial (within a factor 2 of its maximum) at 1215 Å. At this wavelength, and $T = 930$ K, we find that $As_3^+/As_2^+ < 0.85 \times 10^{-3}$.

Now consider the gas phase reaction

$$As_2 + As_4 \rightarrow 2As_3.$$

The equilibrium constant can be written

$$K_{930} = \frac{(As_3)^2}{(As_2)(As_4)} \lesssim \frac{(0.85\times10^{-3})^2}{(1)(0.3)} \lesssim 2.4\times10^{-6}.$$

Hence, $\Delta F^0_{930} = -RT \ln K_{930} \geqslant 23.91$ kcal/mol.

We must now compute the change in free energy functions, $\Delta[-(F^0 - E^0_0)/T]$, at $T = 930$ K. For As_4, which is tetrahedral with an As–As distance of 2.435(4) Å (Ref. 23) and vibrational frequencies given by Ozin,[14] we obtain $-(F^0 - E^0_0)/T = 82.7241$ cal K^{-1} mol^{-1}. For As_2,[19] with $r_e = 2.1026$ Å and $\omega = 429.0$ cm^{-1}, $-(F^0 - E^0_0)/T = 59.0723$ cal K^{-1} mol^{-1}.

For As_3, no spectroscopic information exists, but we can make some plausible estimates. Although the first row analog N_3 is linear, *ab initio* calculations,[24,25] indicate that P_3 is clearly bent. In fact, these calculations lead to a nearly equilateral structure for P_3 in its ground state. The calculated ground state is $^2E''$, which is subject to Jahn–Teller distortion, but apparently[24] this distortion is small. Hence, the electronic contribution to $-(F^0 - E^0_0)/T$ will reflect this degeneracy, which we carry over to As_3. The P–P distance in P_3 calculated by Jones and Hohl,[25] when corrected for their underestimate of this distance in P_2 and P_4, amounts to 2.14 Å. In a configuration interaction calculation of P_3, Murrell *et al.*[24] obtained a P–P distance of ~2.24 Å. We choose an average value, 2.19 ± 0.05 Å, and compare this quantity with the P–P distance in P_4 (2.2228 Å). We apply this ratio to the As–As distance in As_4, and thereby deduce 2.40 ± 0.05 Å as the As–As distance in As_3, which is assumed to be equilateral. For such a structure, the principal moments of inertia are mr^2, $mr^2/2$, and $mr^2/2$, where m is the mass of the atom and r is the distance between atoms. The product of these moments of inertia for As_3 is calculated to be 9.22×10^7 (in units of 10^{-120} gm^3 cm^6). The symmetry number is 6.

According to Burdett and Marsden,[26] the structure of P_3^+ is not very different from P_3. It is calculated to be bent, with an angle of 60°, and a P–P distance of 2.077 Å. It is a closed shell system ($^1A_1'$); the next electron goes into an e' orbital (LUMO), which should be relatively easily removed, i.e., P_3 should have a low ionization potential. Burdett and Marsden[26] calculate ν_1 (a_1') and ν_2 (e') for the equilateral P_3^+, and then correct the calculation by calibration with P_2. Thus their best estimate is $\nu_1 = 643$, $\nu_2 = 463$ cm^{-1}. We assume that the additional e' electron is nonbonding; then using the ratio of ν_1 to $\nu(P_2)$ and ν_2 to $\nu(P_2)$, and applying this ratio to As_2 and As_3, we estimate $\nu_1(As_3) = 354$ cm^{-1} and $\nu_2(As_3) = 255$ cm^{-1}. With these estimated properties, we calculate $-(F^0 - E^0_0)/T$ at our experimental temperature 930 K.

With contributions of 42.820 (translational), 25.157 (rotational), 6.171 (vibrational), and 2.755 (electronic), the total free energy function for As_3 at 930 K becomes 76.903 cal K^{-1} kmol^{-1}. Thus

$$\Delta\left[-\frac{(F^0 - E^0_0)}{T}\right] = 12.009_6 \text{ cal K}^{-1} \text{ mol}^{-1},$$

$$-\Delta F^0_{930} + \Delta E^0_0 = 11.17 \text{ kcal/mol},$$

and hence

$$\Delta E_0 = \Delta H_0 \geqslant 35.1 \text{ kcal/mol}.$$

With the aforementioned $\Delta H^0_{f_0}(As_4) = 38.5 \pm 0.6$ kcal/mol and $\Delta H^0_{f_0}(As_2) = 46.4$ kcal/mol, we finally obtain $\Delta H^0_{f_0}(As_3) \geqslant 60.0$ kcal/mol. Bennett *et al.*[27] have observed a threshold for the process

$$As_4 + e^- \rightarrow As^- + As_3,$$

corresponding to 83.0 ± 2.3 kcal/mol. In their analysis, they subtract 11.4 ± 0.6 kcal/mol, which they infer as excess kinetic and vibrational energy at threshold. Then, using values of $\Delta H^0_{f_0}(As_4) = 36.64 \pm 0.40$ kcal/mol, $\Delta H^0_{f_{298}}(As) = 68.43 \pm 0.6$ kcal/mol and EA (As) $= 17.8 \pm 1.2$ kcal/mol, they obtain $\Delta H^0_{f_{298}}(As_3) = 57.6 \pm 3.9$ kcal/mol. With our current values for $\Delta H^0_{f_{298}}(As_4) = 37.8 \pm 0.6$,[17] $\Delta H^0_{f_{298}}(As_g) = 69.1 \pm 0.4$,

and EA (As) = 18.7 ± 0.7,[28] all in kcal/mol, we obtain $\Delta H^0_{f_{298}}(As_3) = 59.0$ kcal/mol. If we retain the view that this measurement pertains to 298 K, then (with our deduced spectroscopic constants), $\Delta H^0_{f_0}(As_3) = 59.5$ kcal/mol.

This value is fortuitously close to our deduced lower limit [$\Delta H^0_{f_0}(As_3) \geqslant 60.0$ kcal/mol]. One may question the inference and use of an excess energy at threshold. It is not clear that the deduced $\Delta H^0_f(As_3)$ should really refer to 298 K. Nevertheless, we believe that the lower limit for $\Delta H^0_{f_0}(As_3)$ calculated here is much closer to the true value than the upper limit, based on the appearance potential of As^+ from As_4.

In Sec. IV, we arrive at a value of $\Delta H^0_{f_0}(As_3) \approx 63$ kcal/mol. based on semiempirical arguments. When combined with our previously deduced $\Delta H^0_{f_0}(As_3^+) \leqslant 228.7$ kcal/mol, we predict IP (As_3) < 7.32 and $\leqslant 7.19$ eV.

In Table III, we summarize the ionization and appearance potentials of the arsenic species, and compare them with prior literature values.

IV. DISCUSSION

A. Heats of formation and bond energies of Pn clusters

The homonuclear diatomic molecules N_2, P_2, As_2, Sb_2, and Bi_2 have rather well established dissociation energies.[19] Sublimation of P, As, and Sb generates the tetramer in highest abundance, and hence the heats of formation of P_4, As_4, and Sb_4 are fairly well known. Thermochemical studies exist which enable one to convert these heats of formation into atomization energies. Although Bi_4 is a minor component in saturated bismuth vapor, its atomization energy has been measured.[29,30] Apart from van der Waals bonding (i.e., $N_2 \cdot N_2$), N_4 is not believed to be stable. For the trimer, the existing information is rather erratic. The molecule N_3 has been observed spectroscopically.[31] It is linear, with a $^2\Pi_g$ ground state. The molecules Sb_3 (Ref. 32) and Bi_3 (Ref. 29) have been observed in high temperature equilibrium mass spectrometric studies. Thermochemical analysis by second and third law methods enables one to infer values for their heats of formation. Unfortunately, the third law analyses have heretofore assumed linear structures for these species, which we now believe to be bent. We shall discuss the error that is incurred by this assumption shortly. The molecules P_3 and As_3 have not been observed directly, to our knowledge. The available information regarding the stabilities of these trimers is based on electron impact appearance potentials for the processes[27,33]

$$M_4 + e^- \rightarrow M^- + M_3,$$

where M = P, As. The arsenic experiment has already been discussed in Sec. III C. In their analysis of the corresponding phosphorus experiment, Bennett *et al.*[33] were led to the conclusion that the P^- must be formed in its ^1D excited state which, according to calculation, should have a heat of formation essentially equal to that of atomic P (^4S state). Thus their appearance potential for this process, 110.7 ± 2.3 kcal/mol, can be identified with

$$P_4 \rightarrow P_3 + P.$$

Bennett *et al.*[34] state that this threshold does not involve excess kinetic or internal energy. In this manner, they deduce $\Delta H^0_{f_{298}}(P_3) = 59.4 \pm 4.0$ kcal/mol. Gurvich *et al.*,[35] utilizing the same data, obtain $\Delta H^0_{f_{298}}(P_3) = 50.2 \pm 4.8$ kcal/mol. The discrepancy primarily involves a choice of the standard state for phosphorus.[36]

Assuming a linear structure, Gurvich *et al.*[35] have computed the entropy and free energy functions for P_3. We have made corresponding calculations for an equilateral triangular structure, as discussed in Sec. III C. Our values are about 2–3 cal K^{-1} mol^{-1} higher for the triangular than for the linear structure between 298 and 1000 K. This difference is relevant to the third law evaluation of $\Delta H^0_f(Sb_3)$ and $\Delta H^0_f(Bi_3)$, since in both instances[29,32] a linear structure was assumed in estimating the corresponding entropies. We have recalculated the heats of formation of these trimers (see the Appendix), using the original experimental data, but assuming that the trimers have an equilateral triangular structure. The resulting value of $\Delta H^0_{f_0}(Sb_3)$ is 9 kcal/mol higher than previously given, while the revised value of $\Delta H^0_{f_0}(Bi_3)$ is 5.9 kcal/mol higher.

TABLE III. Ionization potentials and appearance potentials for the various As_n species (in eV).

Species	Adiabatic IP	Selected adiabatic higher IP's	Appearance potentials	
As	9.7886 ± 0.0002[a]			
As_2	9.69 ± 0.02	$A\,^2\Sigma_g^+$: 10.238 ± 0.002	$As^+(As_2)$:	13.82 ± 0.08
	9.636(6)[b]	10.230(5)[b]		
	9.52 ± 0.05[c]	10.22[c]		
		$B\,^2\Sigma_u^+$: 15.37		
		15.32[d]		
As_3	< 7.32			
	$\leqslant 7.19$			
As_4	$\leqslant 8.49$	$\tilde{B}\,^2A_1$: 11.017(3)[e]	$As_3^+(As_4)$:	11.23 ± 0.05
	7.83[e]	11.09 ± 0.01[e]		
			$As_2^+(As_4)$:	$12.33_8 \pm 0.02_4$
			$As^+(As_4)$:	15.09 ± 0.05

[a] Reference 20.
[b] Reference 7.
[c] Reference 5.
[d] Reference 4.
[e] Reference 6.

TABLE IV. Heats of formation of pnicogen (Pn) atoms and molecules (kcal/mol).

Species	$\Delta H_{f_0^\circ}(Pn)$	$\Delta H_{f_0^\circ}(Pn_2)$	$\Delta H_{f_0^\circ}(Pn_3)$	$\Delta H_{f_0^\circ}(Pn_4)$
N	112.5 ± 0.1[a]	0	105 ± 4[a]	~0
P	75.42 ± 0.17[a]	34.8 ± 0.3[a]	51.2 ± 4.8[a]	15.83 ± 0.07[a]
As	68.8 ± 0.4[b]	46.3 ± 0.7[b]	(63),[c] 59.5[d]	38.5 ± 0.6[b]
Sb	66.0 ± 1[e]	60.8 ± 1[e]	72.9 ± 2[f]	50.23 ± 0.20[g]
	63.9 ± 0.09[h]	56.8 ± 2.3[h]	71.3 ± 2[f]	51.1 ± 0.6[h]
Bi	50.0 ± 1.5[i]	53.0 ± 1.8[i]	70.0 ± 4.3[j]	59.0 ± 3.4[i]
	49.7 ± 0.4[k]	52.7 ± 0.3[i]	···	58.6 ± 1.0[k]

[a] Reference 35.
[b] These selections are discussed in Ref. 17.
[c] Present work.
[d] Reference 27, reinterpreted (see Sec. III C).
[e] Reference 32.
[f] Reinterpretation of Kordis and Gingerich (Ref. 32) (see the Appendix) using alternative values of $\Delta H_{f_0^\circ}(Sb_2)$ and $\Delta H_{f_0^\circ}(Sb_4)$.
[g] Reference 41.
[h] J. Drowart, S. Smoes, and J. Vanderauwera-Mahieu, J. Chem. Thermodyn. **10**, 453 (1978).
[i] Reference 29.
[j] Reinterpretation of Rovner *et al.* (Ref. 29) (see the Appendix).
[k] Reference 30.

Table IV is a compilation of values for $\Delta H^0_{f_0}(Pn_n)$, where Pn refers to the pnicogens N, P, As, Sb, and Bi, and $n = 1$–4. This table includes the recalculated values of $\Delta H^0_{f_0}(Sb_3)$ and $\Delta H^0_{f_0}(Bi_3)$. Probably the most uncertain quantities in this table are $\Delta H^0_{f_0}(P_3)$ and $\Delta H^0_{f_0}(As_3)$, both of them not observed directly. In Table V, we present the formal energy changes for the processes $Pn_4 \rightarrow Pn_3 + Pn$, $Pn_3 \rightarrow Pn_2 + Pn$, and $Pn_2 \rightarrow Pn + Pn$. The first two processes do not really represent successive bond energies, since considerable rearrangement occurs. Nevertheless, it provides a basis for examining systematic behavior. Next to each "bond energy" is shown the fraction of the average of the three dissociation energies which it represents. With our choice of $\Delta H^0_{f_0}(As_3) \simeq 63$ kcal/mol, there is a relatively smooth progression in this fraction. With $\Delta H^0_{f_0}(As_3) \cong 59$ kcal/mol obtained by Bennett *et al.*,[27] there is a discontinuity at the arsenic position.[37] In Table VI, we calculate the average bond energy for these species, in the spirit of Pauling.[38] As an example, the heat of atomization of P_4 is 285.8 kcal/mol. In going from the tetrahedral structure to free atoms, six bonds are broken. Therefore, the "average bond energy" in P_4 is 47.6 kcal. Similarly, the heat of atomization of P_3, according to Bennett *et al.*,[33] is 175 kcal/mol. If we accept the *ab initio* results,[24,25] in which P_3 is nearly equilateral, three bonds will be broken upon atomization and consequently the average bond energy of P_3 is 58.3 kcal. The average bond energy of P_2 is just $D_0(P_2) = 116.0$ kcal/mol. Also shown in Table VI are two ratios: the average bond energy in Pn_4 to that of the dimer, and the average bond energy in Pn_3 to that of the dimer. In this representation, we see that the average bond energy in Pn_4 and in Pn_3 is about 1/2 that in Pn_2. Formally, the bond in Pn_2 is a triple bond in N_2.[39] The increase in this ratio for the heavier pnicogen systems is attributed to the relative weakness of the triple bond, which in turn is associated with weak π bonding. A manifestation of this abrupt transition in behavior between the first main row in Group IV (C–C bonds) and the heavier members (Si–Si and Ge–Ge bonds) has recently been observed in our laboratory.[40]

B. Photodissociative ionization thresholds from As_4, and their relation to thermochemical thresholds

1. As_3^+ from As_4

In Sec. III A 2, we obtained $\Delta H^0_{f_0}(As_3^+) \leqslant 228.7$ kcal/mol. In Sec. III C, we concluded that $\Delta H^0_{f_0}(As_3) > 60.0$ kcal/mol, and in Sec. IV A, that a value for $\Delta H^0_{f_0}(As_3)$ of 63 kcal/mol was plausible. Therefore, the adiabatic ionization potential of As_3 is < 7.32 eV, and is probably $\leqslant 7.19$ eV.

TABLE V. Dissociation energies of the Pn clusters (kcal/mol) and their fractional components (f).

	P		As		Sb		Bi	
	ΔH_0	f	ΔH_0	f	ΔH_0	f	ΔH_0	f
$Pn_4 \rightarrow Pn_3 + Pn$	110.8	1.16	93.3	1.18	88.7 (84.1)	1.24 (1.23)	61	1.30
$Pn_3 \rightarrow Pn_2 + Pn$	59.0	0.62	52	0.66	53.9 (49.5)	0.76 (0.73)	33	0.70
$Pn_2 \rightarrow Pn + Pn$	116.0	1.21_8	91.3	1.15_8	71.2 (71.0)	1.00 (1.04)	47	1.00

TABLE VI. "Average bond energies" of the Pn clusters (kcal/mol) and their fractional components (f).

	P		As		Sb		Bi	
	ΔH_0	f	ΔH_0	f	ΔH_0	f	ΔH_0	f
Pn_4[a]	47.6	0.41	39.4	0.43	35.6(34.1)	0.50(.48)	23.5	0.50
Pn_3[b]	58.3	0.50	47.8	0.52	41.7(40.1)	0.59(.56)	26.7	0.57
Pn_2	116.0	1.00	91.3	1.00	71.2(71.0)	1.00	47	1.00

[a]Average bond energy of Pn_4 = 1/6 of atomization energy.
[b]Average bond energy of Pn_3 = 1/3 of atomization energy.

2. As_2^+ from As_4

In Sec. III A 3, we showed that the appearance potential of As_2^+ from As_4 (12.338 ± 0.024 eV), together with the ionization potential of As_2 (9.69 ± 0.02 eV) implied $D_0(As_2-As_2) \leqslant 61.0 \pm 0.8$ kcal/mol. Thermochemical studies since 1973 have yielded lower values, the most accurate and probable being around 54 kcal/mol. This latter value has been assumed in the present article, and hence our higher threshold was attributed to a kinetic shift in the dissociative ionization process. Thermochemical studies prior to 1973, summarized by Hultgren *et al.*[41] have consistently yielded higher values. The average adopted by Hultgren *et al.* was 69 kcal/mol. Thus, although the more recent studies have taken precautions to eliminate re-evaporation of As_4, which apparently plagued the earlier studies, it may still be possible that the true value of $D_0(As_2-As_2)$ is somewhat larger than 54 kcal/mol, but it is definitely $\leqslant 61.0$ kcal/mol. In this regard, we note that the kinetic shift observed in P_2^+ from P_4 is much smaller than that inferred from As_2^+ (As_4).

C. The autoionizing Rydberg series in As_2

1. The series converging to $A\,^2\Sigma_g^+$

It will be recalled (Sec. III B) that two series, dubbed a strong and a weak series, were observed. For a given value of the principal quantum number n, the stronger series was lower in energy. On the basis of its strength, it was assigned as an $np\pi\,^1\Pi_u$ series, whereas the weaker one was assigned to $np\sigma\,^1\Sigma_u^+$.

Carroll and Mitchell[18] have observed related series in a photoabsorption study of P_2, which we have also observed in photoionization.[9] They identified two stronger series, which they termed $np\sigma_u$, G_n, $^1\Sigma_u^+$, and $np\pi_u$, H_n, $^1\Pi_u$. (In addition, they observed weaker series going to the same limit, which they attributed to nf Rydberg electrons). The first two members of the G_n series had previously been analyzed by Creutzberg.[42] They were found to be of species $^1\Sigma_u^+$. In P_2, the G_n series lies below the H_n series. Further evidence that the G_n series is to be identified with $np\sigma_u$ comes from the measured vibrational interval in its first member (686 cm^{-1}), which is lower than that of the ion core $A\,^2\Sigma_g^+$ (733 cm^{-1}), an observation consistent with the slightly antibonding character of $np\sigma_u$.

With the present resolution, we have neither vibrational nor rotational information on the corresponding series in As_2. The analogy to P_2 is a stronger basis for assignment than the relative intensities of the series, in our judgment, and hence the stronger, lower energy series is designated $np\sigma_u\,^1\Sigma_u^+$.

2. The window resonance series in As_2

In Sec. III B we described a window resonance series which was attributed to the process

$$\cdots(\sigma_g 4s)^2(\sigma_u 4s)^2(\sigma_g 4p)^2(\pi_u 4p)^4\ {}^1\Sigma_g^+ + h\nu$$
$$\rightarrow \cdots(\sigma_g 4s)^2\sigma_u 4s(\sigma_g 4p)^2(\pi_u 4p)^4\ {}^2\Sigma_u^+ ns.$$

We identified the limit with the $B\,^2\Sigma_u^+$ state of As_2^+.

Carroll and Mitchell[18] have observed a similar window resonance series in their study of the photoabsorption spectrum of P_2. They attributed their series to the two-electron transitions

$$\cdots(\sigma_g 3s)^2(\sigma_u 3s)^2(\sigma_g 3p)^2(\pi_u 3p)^4\ {}^1\Sigma_g^+ + h\nu$$
$$\rightarrow \cdots(\sigma_g 3s)^2(\sigma_u 3s)^2\sigma_g 3p(\pi_u 3p)^3\pi_g 3p\ {}^2\Sigma_u^+ ns.$$

They thought that it was analogous to the series in N_2 observed by Codling[43] which converged on the $C\,^2\Sigma_u^+$ state of N_2^+. However, Bulgin *et al.*[44] showed that the series limit closely corresponds with a weak peak in their photoelectron spectrum which they attributed to the single electron ejection process $(\sigma_u 3s)^{-1}$, and which they called the $B\,^2\Sigma_u^+$ state of P_2^+. Our assignment for the window resonance series in As_2 is analogous to the interpretation of the window resonance series in P_2 proposed by Bulgin *et al.*[44]

D. Application to cluster studies

To our knowledge, studies of large clusters of arsenic have not yet been reported. However, there have been several studies of antimony and bismuth clusters. Antimony, like arsenic, sublimes predominantly as tetramer.[41] When the antimony vapor from an oven is coexpanded with He through a nozzle, only clusters of tetramers (Sb_{4n}) are formed,[45-47] and observed as the corresponding parent ions by low energy electron impact. Bismuth vaporizes primarily as monomer and dimer, with very small abundances of trimer and tetramer.[41] The corresponding expansion cooled spectrum at 10 eV electron impact energy reveals peaks at essentially all Bi_n^+ in a broad distribution.[45,47,48] Both of these observations can be plausibly inferred as condensation and growth from the initial vapor composition leaving the oven.

If, alternatively, the cations resulting directly from laser irradiation of a surface (Sb or Bi) are examined, rather different mass spectra are observed. For both Sb and Bi, the

prominent ions are Pn^+, Pn_3^+, Pn_4^+, Pn_5^+, and Pn_7^+.[49] Geusic *et al.*[50] have also studied the photofragmentation of mass selected Sb_n^+ and Bi_n^+ with 248 nm laser radiation. Here again, the odd numbered cluster ions tend to dominate. For example, Bi_5^+ dissociates entirely to $Bi_3^+ + Bi_2$; Sb_6^+ dissociates primarily to $Sb_3^+ + Sb_3$ (61%), but also to $Sb_4^+ + Sb_2$. Geusic *et al.*[50] conclude that the "magic number patterns especially favoring the three-, five-, and seven-atom species ··· suggest that magic numbers are strongly influenced by cluster stability." Elsewhere, they note that these stabilities are consistent with Wade's Rules,[51] which described the optimum number of skeletal electrons corresponding to different polyhedral structures.

The data assembled in the present work provides a beginning in the understanding of the thermochemistry of these systems. For example, let us assume that laser induced vaporization of Sb_n^+ cations is a process governed by local thermodynamic equilibrium. With that assumption, the abundance of a given cation species observed will be higher if its heat of formation (rigorously, its free energy of formation) is lower. The heats of formation are (in kcal/mol): Sb^+ ~264, Sb_2^+ ~256, Sb_3^+ ~219,[52] Sb_4^+ ~219. Within our limited range of knowledge, we would predict that Sb_3^+ and Sb_4^+ would dominate over Sb^+ and Sb_2^+. In fact, Sb^+ is observed to be comparable to Sb_3^+ and Sb_4^+, with Sb_2^+ about 1/3 as large.[49] The observed intensity of Sb^+ suggests that other effects are influencing the cation abundance besides ionic stability.

The photofragmentation of Sb_6^+ can lead to the following binary fragments [the sum of the fragment heats of formation (kcal/mol) are indicated in parentheses]

$$Sb_6^+ + h\nu \rightarrow Sb_4^+ + Sb_2\ (\sim 279),$$
$$\rightarrow Sb_3^+ + Sb_3\ (\sim 289),$$
$$\rightarrow Sb_2^+ + Sb_4\ (\sim 313).$$

The fragments $(Sb_5^+ + Sb)$ and $(Sb^+ + Sb_5)$ should also be considered. We have no information on Sb_5 and Sb_5^+; however, they are not observed in the photofragmentation spectrum. From the available thermochemistry, we would predict that Sb_4^+ should be the dominant photofragment, followed by Sb_3^+, with Sb_2^+ much weaker. In fact, while Sb_2^+ is absent, Sb_3^+ is twice as abundant as Sb_4^+. One may argue that the thermochemistry is not that well established. In fact, the heats of formation of $(Sb_4^+ + Sb_2)$ are now rather well known. The combined heats of formation of $(Sb_3^+ + Sb_3)$ are based on our third law derived value for $\Delta H_f^0\ (Sb_3)$, and a rather low ionization potential (6.34 eV, compared to an electron impact value of 7.50 ± 0.13 eV).[51] A lower value of $\Delta H_f^0\ (Sb_3)$ was deduced by Kordis and Gingerich[32] from their data, based on a linear structure, but this structure is unlikely to be the more stable one, based on the trend of currently available calculations.[24,25]

For the decomposition of Sb_5^+, the thermochemistry is in qualitative agreement with the observations. The combined heats of formation of $(Sb_3^+ + Sb_2)$ amount to ~279 kcal/mol, whereas the ΔH_{f° sum of $(Sb_4^+ + Sb)$ is ~285 kcal/mol. The observations favor Sb_3^+ over Sb_4^+ by about 3:2. The combined heats of formation of the other products $(Sb^+ + Sb_4$, $\Delta H_{f^\circ\text{sum}}$, ~315 kcal/mol, $Sb_2^+ + Sb_3$, $\Delta H_{f^\circ\text{sum}}$ ~328 kcal/mol) are much higher, and they are not observed.

Since we know $\Delta H_{f0}^0\ (Sb_4^+)$, we can calculate the actual endothermicity of various dissociation processes. Thus formation of $Sb_2^+ + Sb_2$ is endothermic by ~97 kcal, while formation of the products $Sb_3^+ + Sb$ requires only ~66 kcal. Absorption of a 248 nm photon excites the Sb_4^+ by 115 kcal, which is well above either threshold. The observations favor Sb_3^+ over Sb_2^+ by 3:1.

There are several confusing statements in the antimony and bismuth cluster literature which we hope that the current research has resolved. Geusic *et al.*[49] state that they do not observe photoionization of antimony atom, dimer, and trimer because all three have ionization potentials greater than the photoionizing laser energy 7.9 eV. While this is true for Sb (IP = 8.609 eV) (Ref. 53) and Sb_2 (IP = 8.5 eV),[7] we infer IP (Sb_3) to be ~6.34 eV, and even the electron impact value (7.50 ± 0.13 eV) (Ref. 52) is lower. The Sb_3^+ was not observed because there was too little Sb_3 in the vapor. Rayane *et al.*[47] are surprised to observe the process $Sb_4^+ \rightarrow Sb_2^+ + Sb_2$, believing that it indicates a nonstatistical distribution of the energy in Sb_4^+ probably due to strong molecular effects. On the basis of sodium cluster ion decomposition, they conclude that when the energy is statistically distributed, successive evaporation is more probable than fission. We have seen (above) that, although $Sb_3^+ + Sb$ is energetically favored over $Sb_2^+ + Sb_2$, both can occur if sufficient energy resides in Sb_4. Also, the present photoionization data reveal an onset for $As_3^+\ (As_4)$, followed by an onset for $As_2^+\ (As_4)$. Similar behavior is observed in the photodissociation of P_4.[8] There is no apparent reason to question the statistical nature of both processes.

Brechignac *et al.*[54] have recently reported the photoionization of antimony clusters between 25–120 eV, using synchrotron radiation. The clusters were prepared by the method described initially by Sattler *et al.*,[45] i.e., the antimony vapor effusing from an oven is cooled by coexpansion with helium. Under these conditions, several studies[45–47] have shown that the clusters consist of Sb_{4n}, with $n = 1, 2, 3$, etc. The dominant photoionization cross sections in the energy domain studied by these authors are attributable to the atomiclike $4d \rightarrow np$, and especially the $4d \rightarrow \epsilon f$ transitions. Brechignac *et al.*[54] observe the large $4d \rightarrow \epsilon f$ cross sections in the Sb_5^+, Sb_6^+, Sb_7^+, Sb_9^+, Sb_{10}^+, Sb_{11}^+, etc., channels, but not in the Sb_8^+, Sb_{12}^+, Sb_{16}^+, etc., channels. In Sb_4^+, the $4d \rightarrow \epsilon f$ region is more evident than in the other Sb_{4n}^+, but less than in the other channels. The authors state that Sb^+ is not observed, but nothing is said about Sb_2^+ and Sb_3^+. The authors conclude that the apparent absence of the $4d \rightarrow \epsilon f$ transition in the Sb_{4n}^+ $(n > 1)$ channels, and its presence in the other channels represents "··· a spectacular dependence (of this resonance) on cluster size which points to a strong modification of the potential inside the constituent atoms." Fragmentation of the photoionized clusters is ruled out as a dominant mechanism because "the relaxation of the electronic excitation into vibration would be much more efficient for Sb_{4n}

clusters than for the other clusters," which seemed unlikely.

From the evidence presented, we favor a different interpretation. The distribution of neutral clusters is assumed to be Sb_{4n}, $n = 1, 2, 3$, etc. Photoionization above the $(4d)^{-1}$ onset (above ~ 40 eV) should form Sb_{4n}^+ with a $4d$ hole, on a time scale of $\sim 10^{-15}$ s. Auger transitions should rapidly follow, creating Sb_{4n} doubly or multiply charged. These charged clusters should undergo Coulomb explosion in perhaps several channels. The most abundant channels may still be the thermodynamically favored ones, which will tend to be the odd numbers, since these singly charged ions will be more stable. We have seen that As_3^+, (and presumably Sb_3^+) is a closed shell structure, the corresponding neutrals having a low ionization potential due to the presence of a single electron in the next higher shell. Although our evidence for Sb_5^+, Sb_7^+, etc., is more speculative, there is some support from the aforementioned direct laser vaporization of ions,[49] which displays higher abundance for the odd numbered clusters. In this scenario, the Sb_{4n} species do indeed absorb strongly in the $4d \rightarrow \epsilon f$ region, but the absorption cross section manifests itself in the resulting fragments. No unusual relaxation of electronic excitation into vibration is required.

Brechignac *et al.*[54] have performed another experiment to support their contention. They have "changed the nucleation conditions, i.e., oven and helium temperatures," which they claim will shift the cluster distribution to odd numbered clusters. They refer to Geusic *et al.*,[49] who observed odd-numbered clusters by direct laser vaporization. Changing the oven temperature should only increase or decrease the Sb_4 intensity, without adding any significant abundance of other species. Changing the helium temperature should influence the degree of clustering of the Sb_4 species, without introducing odd numbered clusters. Presumably due to the limitation of their monochromator, Brechignac *et al.*[54] do not measure this distribution with low energy photons, where fragmentation would be minimal. Instead, they measure the photoionization mass spectrum with the broad photon energy distribution reflected by the grating at zeroth order, which will still emphasize fragmentation processes, and make the odd numbered cluster ions appear prominently, although their abundance as neutrals may be negligible. (They also mention that the same relative intensities are observed with electron impact ionization, but do not state the electron energy used.) We have no explanation for their observations that the changed nucleation conditions result in an Sb_8^+ photoion yield curve with a prominent $4d \rightarrow \epsilon f$ resonance, whereas Sb_8^+ under the original nucleation conditions did not.

After completion of the present manuscript, we became aware of a recently published set of *ab initio* calculations performed on P_3, As_3, Sb_3, and Bi_3 and their cations by Balasubramanian *et al.*[55] These calculations were performed by both complete active space self-consistent field (CASSCF) and multireference configuration interaction (MRCI) methods. These authors conclude that in all cases, the trimers are triangular, and nearly equilateral, as we had assumed. Their calculated internuclear distances [r(As–As) = 2.35 Å, r(Sb–Sb) = 2.76 Å, r(Bi–Bi) = 2.94 Å] are close to our estimated distances [r(As–As) = 2.40 Å, r(Sb–Sb) = 2.67 Å, r(Bi–Bi) = 2.99 Å]. For Sb_3, where the largest discrepancy occurs, the net effect of using the calculated distance is to increase our inferred $\Delta H_{f_0}^0(Sb_3)$ by 0.2 kcal/mol. Each of the neutral states is slightly Jahn–Teller split, as assumed. For Bi_3, the spin–orbit splitting is larger than the Jahn–Teller splitting. Their calculated IP for As_3 (7.1 eV) is remarkably close to our derived value ($\leqslant$7.19 eV). Their calculated IP for P_3 (7.31 eV) is lower than that given by Smets *et al.*[8] (7.85 ± 0.05 eV), but the latter value is based on a somewhat uncertain $\Delta H_f^0(P_3)$ reported by Bennett *et al.*[33] Balasubramanian *et al.* obtain two different values for IP (Sb_3): 6.5 eV by CASSCF, and 7.1 eV by MRCI. They favor the higher value, because it is closer to the experimental electron impact[52] result, 7.50 ± 0.13 eV. However, our scaled estimate, 6.34 eV, is closer to their CASSCF result.

For the dissociation process $Pn_3 \rightarrow Pn_2 + Pn$, Balasubramanian *et al.* obtain 33, 30, 28.8, and 23 kcal/mol for Pn = P, As, Sb, and Bi, respectively, compared to the values given in Table V, i.e., 59, 52, 53.9, (49.5), and 33 kcal/mol. For the atomization energies of the trimers, they calculate 127, 122, 101.5, and 69 kcal/mol, whereas our derived values implicitly given in Table VI are 175.0, 143.4, 125 (120), and 80 kcal/mol for P_3, As_3, Sb_3, and Bi_3. Hence, in every case the calculated dissociation energies fall below the experimental values, a deviation recognized by Balasubramanian *et al.*[55] and attributed to missing correlation energy. The atomization energies for As_3, Sb_3, and Bi_3 deduced in the present work are uniformly lower than prior experimental values (primarily due to the recalculated entropies of the trimers), and consequently, closer to the *ab initio* calculated values, although the discrepancies are still substantial. More recently, we have developed semiempirical expressions utilizing the known heats of formation of dimers and tetramers to estimate the heats of formation of the trimers, in very good agreement with the currently deduced experimental values.[56]

This work was supported by the U.S. Department of Energy, Office of Basic Energy Sciences, under Contract No. W-31-109-ENG-38.

APPENDIX

(A) Our goal is to calculate $\Delta H_{f_0}^0(Sb_3)$. We separate the problem into (1) determination of a free energy change and (2) determination of a change in free energy functions.

(1) Kordis and Gingerich[32] in their Table I give measured relative intensities of Sb_2^+, Sb_3^+, and Sb_4^+ at 11 temperatures. Consider the equilibrium $Sb_2 + Sb_4 \rightarrow 2Sb_3$. The equilibrium constant, $K = (Sb_3^+)^2/(Sb_2^+)(Sb_4^+)$ is independent of pressure. The Knudsen cell-mass spectrometric dependence on temperature, i.e., $P(Sb_n) = k_n I(Sb_n^+) T$, cancels out. The assumptions regarding relative ionization cross sections and ion multiplier corrections also cancel out, for practical purposes. Hence, the equilibrium constant (and therefore ΔF_T^0 for the reaction) can be calculated directly from the relative ion intensities.

(2) Free energy functions

(a) Sb_2. With $r_e = 2.3415$ Å and $\omega = 269.7\ cm^{-1}$ from Huber and Herzberg,[19] the calculation of $-(F^0 - E_0^0)/T$ is straightforward.

(b) Sb_4. We assume a tetrahedral structure, as has been determined[11] for P_4 and As_4. The ratio of P–P distance in P_4 (Ref. 11) to P–P distance in P_2 (Ref. 19) is 1.174. The corresponding ratio in arsenic is 1.158. We apply this latter ratio to antimony. Then from $r_e(Sb_2) = 2.3415$ Å,[19] we deduce $r(Sb_4) = 2.71$ Å. Each principal moment of inertia in these tetrahedral species is given by $I_{xx} = I_{yy} = I_{zz} = mr^2$, where m is the mass of the atom, and r is the interatom distance. Hence, $I_{xx}(Sb_4) = 1486 \times 10^{-40}$ gm cm^2, $\ln(I_{xx} I_{yy} I_{zz}) = 21.9125$. With $\sigma = 12$, this completes the parameters for the translational and rotational contribution to $-(F^0 - E_0^0)/T$ for Sb_4. The vibrational frequencies are scaled by noting the ratios of the three frequencies in P_4 to that in P_2, and also the corresponding ratios in As_4 and As_2, then applying those ratios to Sb_2. In this way, we obtain $\nu_1 = 210$, $\nu_2(2) = 127$, $\nu_3(3) = 160.7\ cm^{-1}$ from the phosphorus base, and $\nu_1 = 213$, $\nu_2(2) = 125.7$, $\nu_3(3) = 157.2\ cm^{-1}$ from the arsenic data. The two scalings yield substantially the same parameters for evaluating the vibrational contribution. There is no electronic contribution.

(c) Sb_3. We assume an equilateral triangular structure. For P_3, the *ab initio* calculations indicate a ^2E ground state, subject to Jahn–Teller distortion. In P_3, the calculated distortion is mild, and we assume this behavior persists in Sb_3. The Sb–Sb distance in Sb_3 is scaled by the ratio of the calculated P–P distance in P_3 (2.19 ± 0.05 Å) to the measured P–P distance in P_4 (2.2228 Å). This ratio, applied to our inferred Sb–Sb distance in Sb_4, yields $r(Sb_3) = 2.67$ Å. The vibrational frequencies of Sb_3 are scaled from the calculated P_3 frequencies and known P_2 frequency, yielding $\nu_1 = 222\ cm^{-1}$ and $\nu_2(2) = 160\ cm^{-1}$. The remainder of the calculation follows the pattern given in Sec. III C for As_3.

(3) Calculation of $\Delta H_{f_0}^0(Sb_3)$

From ΔF^0 and $\Delta[-(F^0 - E_0^0)/T]$ for the disproportionation reaction, we obtain $\Delta E_0^0 \equiv \Delta H_0^0$. The average ΔE_0^0 for all 11 temperatures is 34.33 kcal/mol. For the four highest intensity points of Sb_3^+, the average is 34.98 kcal/mol. We choose 34.7 ± 0.4 kcal/mol. Then, taking $\Delta H_{f_0}^0(Sb_2) = 60.8 \pm 1$ kcal/mol and $\Delta H_{f_0}^0(Sb_4) = 50.23 \pm 0.20$ kcal/mol (see Table IV), we obtain $\Delta H_{f_0}^0(Sb_3) = 72.9 \pm 2$ kcal/mol. Alternatively, using $\Delta H_{f_0}^0(Sb_2)$ and $\Delta H_{f_0}^0(Sb_4)$ from Drowart *et al.* (also given in Table IV), we obtain $\Delta H_{f_0}^0(Sb_3) = 71.3 \pm 2$ kcal/mol.

(B) Calculation of a revised value for $\Delta H_{f_0}^0(Bi_3)$

Rovner *et al.*[29] have reported $\Delta H_{f_0}^0(Bi_3) = 64.1 \pm 4.3$ kcal/mol, based upon the gas phase reaction $Bi_3 \rightarrow 3Bi$. In their third law evaluation, they estimated the free energy function of Bi_3 assuming a linear structure. They obtained $-(F^0 - E_0^0)/T = 84.57$ cal K^{-1} mol^{-1} at 1000 K. Making the same scaling assumptions as used for As_3 and Sb_3, we obtain $r(Bi_3) = 2.987$ Å, $\nu_1 = 127\ cm^{-1}$ and $\nu_2(2) = 91.5\ cm^{-1}$. At 1000 K, this yields $-(F^0 - E_0^0/T) = 90.42$ cal K^{-1} mol^{-1}. The larger entropy of 5.85 cal K^{-1} mol^{-1} decreases the ΔH_{1000} of the above reaction by 5.85 kcal/mol, i.e., from 85.9 to 80.0 kcal/mol. This increases $\Delta H_{f_0}^0(Sb_3)$ from 64.1 to 70.0 kcal/mol.

[1] H. Bock and H. Müller, Inorg. Chem. **23**, 4365 (1984).
[2] See, for example, J. C. Garcia, C. Neri, and J. Massies, J. Cryst. Growth **98**, 511 (1989), and references therein.
[3] J. Berkowitz, in Proceedings of the IV Intern. Conf. on Vac. Ultraviolet Radiation Physics, edited by E. E. Koch, R. Haensel, and C. Kunz (Pergamon, Berlin, 1974), p. 116.
[4] S. Elbel, H. Tom Dieck, and H. Walther, Inorg. Chim. Acta **53**, L101 (1981).
[5] J. M. Dyke, S. Elbel, A. Morris, and J. C. H. Stevens, J. Chem. Soc. Faraday Trans. 2 **82**, 637 (1986).
[6] L.-S. Wang, B. Niu, Y. T. Lee, D. A. Shirley, E. Ghelichkani, and E. R. Grant, J. Chem. Phys. **93**, 6318, 6327 (1990).
[7] L.-S. Wang, Y. T. Lee, D. A. Shirley, K. Balasubramanian, and P. Feng, J. Chem. Phys. **93**, 6310 (1990).
[8] J. Smets, P. Coppens, and J. Drowart, Chem. Phys. **20**, 243 (1977).
[9] J. Berkowitz and B. Ruscic, in *Vacuum Ultraviolet Photionization and Photodissociation of Molecules and Clusters*, edited by C. Y. Ng (World Scientific, Singapore, 1991), p. 37.
[10] J. Berkowitz, J. P. Greene, and H. Cho, J. Phys. B **20**, 4409 (1987).
[11] *Landoldt–Bornstein Tables, New Series, Group II. Atomic and Molecular Physics*, Vol. 7, Structure Data of Free Polyatomic Molecules (Springer, Berlin, 1976), p. 18; Vol. 15 (1987), p. 135.
[12] C. R. Brundle, N. A. Kuebler, M. B. Robin, and H. Basch, Inorg. Chem. **11**, 20 (1972).
[13] S. Evans, P. J. Joachim, A. F. Orchard, and D. W. Turner, Int. J. Mass Spectron. Ion Phys. **9**, 41 (1972).
[14] The vibrational frequencies of As_4, $\nu_1(a_1) = 340\ cm^{-1}$, $\nu_2(e) = 200\ cm^{-1}$, and $\nu_3(f_2) = 250\ cm^{-1}$ are taken from G. A. Ozin, Chem. Commun. **1969**, 1325.
[15] P. M. Guyon and J. Berkowitz, J. Chem. Phys. **54**, 1814 (1971).
[16] We take the average of two results: $\Delta H_{f298}^0(As_4) = 38.54 \pm 0.10$ kcal/mol from C. C. Herrick and R. C. Feber, J. Phys. Chem. **72**, 1102 (1968), and $\Delta H_{f298}^0(As_4) = 37.34 \pm 0.02$ kcal/mol from H. Rau, J. Chem. Thermodyn. **7**, 27 (1975). The result, 37.8 ± 0.6 kcal/mol, becomes 38.5 ± 0.6 kcal/mol at 0 K.
[17] See, J. Berkowitz, J. Chem. Phys. **89**, 7065 (1988).
[18] P. K. Carroll and P. I. Mitchell, Proc. R. Soc. London, Ser. A **342**, 93 (1975).
[19] K. P. Huber and G. Herzberg, *Molecular Spectra and Molecular Structure IV. Constants of Diatomic Molecules* (Van Nostrand Reinhold, New York, 1979).
[20] K. S. Bhatia and W. E. Jones, Can. J. Phys. **49**, 1773 (1971).
[21] C. E. Theodosiou, M. Inokuti, and S. T. Manson, At. Data **35**, 473 (1986).
[22] G. D. Kinzer and G. M. Almy, Phys. Rev. **52**, 814 (1937).
[23] Y. Morino, T. Ukaji, and T. Ito, Bull. Chem. Soc. Jpn. **39**, 64 (1966).
[24] N. N. Murrell, O. Novaro, S. Castillo, and V. Saunders, Chem. Phys. Lett. **90**, 421 (1982).
[25] R. O. Jones and D. Hohl, J. Chem. Phys. **92**, 6710 (1990).
[26] J. K. Burdett and C. J. Marsden, New J. Chem. **12**, 797 (1988).
[27] S. L. Bennett, J. L. Margrave, J. L. Franklin, and J. E. Hudson, J. Chem. Phys. **59**, 5814 (1973).
[28] H. Hotop and W. C. Lineberger, J. Phys. Chem. Ref. Data **14**, 731 (1985).
[29] L. Rovner, A. Drowart, and J. Drowart, Trans. Faraday Soc. **63**, 2906 (1967).
[30] F. J. Kohl, O. M. Uy, and K. D. Carlson, J. Chem. Phys. **47**, 2667 (1967).
[31] A. E. Douglas and W. Jones, Can. J. Phys. **43**, 2216 (1965).
[32] J. Kordis and K. A. Gingerich, J. Chem. Phys. **58**, 5141 (1973).
[33] S. L. Bennett, J. L. Margrave, and J. L. Franklin, J. Chem. Phys. **61**, 1647 (1974).
[34] E. Clementi, A. D. McLean, R. L. Raimondi, and M. Yoshimine, Phys. Rev. A **133**, 1274 (1964).
[35] L. V. Gurvich, I. V. Veyts, and C. B. Alcock, *Thermodynamic Properties of Individual Substances*, Vol. 1, 4th ed. (Hemisphere, New York, 1989).

[36] In an earlier (1971) edition, the JANAF tables chose red phosphorus as a standard state. In the 3rd edition (1985) they have switched to white phosphorus, the standard state adopted by Glushko *et al.* and Lias *et al.* Bennett *et al.* used the 1971 JANAF convention. We implicitly use the new standard in the present work.

[37] V. A. Titov, T. P. Chusova, and G. A. Kokovin, Izvest. Sibirs. Otdel. Akad. Nauk SSSR, Ser. Khim. Nauk. **3**, 42 (1983) measured the dependence of the total pressure in unsaturated arsenic vapor on temperature and initial weight or concentration. They fitted their data assuming three equilibria: $2As \rightarrow As_2$, $2As_2 \rightarrow As_4$ and $3As_2 \rightarrow 2As_3$. To minimize the variables, they fixed $S^0_{298}(As_2)$ and $\Delta H^0_{f298}(As_4)$, both well known. From the fit to their data, they deduced $\Delta H^0_{f298}(As_3) \cong 43$ kcal/mol, far below our lower limit, and that given by Bennett *et al.* (Ref. 27).

[38] L. Pauling, *The Nature of the Chemical Bond* (Cornell University, Ithaca, 1960).

[39] B. Ruscic and J. Berkowitz, J. Chem. Phys. **95**, 4378 (1991).

[40] B. Ruscic and J. Berkowitz, J. Chem. Phys. **95**, 2416 (1991).

[41] R. Hultgren, P. D. Desai, D. T. Hawkins, M. Gleiser, K. K. Kelley, and D. Wagman, *Selected Values of the Thermodynamic Properties of the Elements* (Amer. Soc. for Metals, Metals Park, 1973).

[42] F. Creutzberg, Can. J. Phys. **44**. 1583 (1966).

[43] K. Codling, Astrophys. J. **143**, 552 (1966).

[44] D. K. Bulgin, J. M. Dyke, and A. Morris, J. Chem. Soc. Faraday Trans. 2 **72**, 2225 (1976).

[45] K. Sattler, J. Mühlbach, and E. Reckagel, Phys. Rev. Lett. **45**, 821 (1980).

[46] K. Sattler, J. Mühlbach, P. Pfau, and E. Recknagel, Phys. Lett. A **87**, 418 (1982).

[47] D. Rayane, P. Melinon, B. Tribollet, B. Cabaud, A. Hoareau, and M. Broyer, J. Chem. Phys. **91**, 3100 (1989).

[48] R. E. Walstedt and R. F. Bell, Phys. Rev. A **33**, 2830 (1986).

[49] M. E. Geusic, R. R. Freeman, and M. A. Duncan, J. Chem. Phys. **89**, 163 (1988).

[50] M. E. Geusic, R. R. Freedman, and M. A. Duncan, J. Chem. Phys. **88**, 163 (1988).

[51] K. Wade, Adv. Inorg. Chem. Radiochem. **18**, 1 (1976).

[52] We estimate the ionization potential of Sb_3 by scaling from P_3 and As_3. Thus taking IP $(P_3) = 7.85 \pm 0.05$ eV from Ref. 8, and IP $(P_2) = 10.516$ eV from Ref. 9, the ratio is 0.746. From the present work, we obtain IP $(As_3) < 7.19$ eV and IP $(As_2) = 9.69$ eV, giving a ratio of IP's of 0.742. Applying this ratio to IP $(Sb_2) = 8.5$ eV (from Ref. 7) yields an estimate for IP $(Sb_3) = 6.34$ eV. An ionization potential for Sb_3 of 7.50 ± 0.13 eV has been reported by B. Cabaud, A. Hoareau, P. Nounou, and R. Uzan, Int. J. Mass Spectrom. Ion Phys. **11**, 157 (1973), by electron impact ionization. Such measurements are often too high.

[53] Y. N. Joshi, V. N. Sarma, and Th. A. M. van Kleef, Physica C **125**, 127 (1984).

[54] C. Brechignac, M. Broyer, Ph. Cahuzac, M. de Frutos, P. Labastie, and J.-Ph. Roux, Phys. Rev. Lett. **67**, 1222 (1991).

[55] K. Balasubramanian, K. Sumathi, and D. Dai, J. Chem. Phys. **95**, 3494 (1991).

[56] B. Ruscic, R. K. Yoo, and J. Berkowitz (to be published).

[57] J. Berkowitz, B. Ruscic, and R. K. Yoo, Comments At. Mol. Phys. (submitted).